



ESCAPING DYNAMICS IN THE PRESENCE OF DISSIPATION AND NOISE IN SCATTERING SYSTEMS

JESÚS M. SEOANE* and MIGUEL A. F. SANJUÁN†
*Departamento de Física, Universidad Rey Juan Carlos,
Tulipán s/n, Móstoles, Madrid 28933, Spain*
*jesus.seoane@urjc.es
†miguel.sanjuán@urjc.es

Received February 26, 2009

Dedicated to the memory of Valery S. Melnik

Chaotic scattering in open Hamiltonian systems is a problem of fundamental interest with applications in several branches of physics. In this paper we analyze the effects of adding external perturbations such as dissipation and noise in chaotic scattering phenomena. Our main result is the exponential decay rate of the particles in the scattering region when the system is affected by dissipation and noise. In the case of dissipation the particles escape more slowly from the scattering region than in the conservative case. However, in the noisy case, the particles escape faster from the scattering region as compared to the noiseless case. Moreover, we analyze the fractal dimension of the set of singularities of the scattering function for the dissipative and the conservative cases. As a result of our analysis we have found that a scaling law exists between the exponential decay rate of the particles and the dissipative parameter, and that the fractal dimension for the noisy case is the unity.

Keywords: Fractals; chaotic scattering; noise.

1. Introduction

The phenomenon of chaotic scattering in Hamiltonian systems in the presence of both dissipation and noise is analyzed in this paper. Most previous works on classical chaotic scattering had focused on purely conservative (Hamiltonian) systems [Jung, 1986; Hénon, 1988; Bleher *et al.*, 1990; Ding *et al.*, 1990; Ott & Tél, 1993]. More recently, the effects of both, dissipation and noise, on chaotic scattering have been addressed [Motter & Lai, 2001; Seoane *et al.*, 2006; Seoane *et al.*, 2007; Seoane & Sanjuán, 2008]. A commonly studied setting is the particle motion in a potential field consisting of a group of potential hills [Bleher *et al.*, 1990; Ding *et al.*, 1990]. In general, there exists a

region where interactions between scattering particles and the potential occur, whereas outside the region, the potential is negligible so that the particle motions are essentially free. This region is often called the *scattering region* [Jung, 1986; Hénon, 1988; Bleher *et al.*, 1990; Ding *et al.*, 1990; Ott & Tél, 1993]. For many potential functions of physical interest, the corresponding classical Hamilton's equations of motion are nonlinear, rendering possible chaotic dynamics in the scattering region. Since the system is open, the region necessarily possesses “exits” for particles to enter and to escape. That is, particles from far away can enter the scattering region through one of the exits, experience chaotic dynamics in the region due to the interaction with the potential, and then exit the region

through the same or a different channel. Because of the chaotic dynamics in the scattering region, particles with slightly different initial conditions (e.g. initial positions and momenta) can experience different paths in the region and, consequently, they can spend drastically different times inside and may exit through different exits in completely different directions. It is in this sense of sensitive dependence of the outcome of the scattering trajectory on the initial condition that the scattering becomes chaotic. In the past two decades or so, physical situations where chaotic scattering is relevant were identified, which include celestial mechanics [Boyd & McMillian, 1993], charged particle motions in electric and magnetic fields [Chernikov & Schmidt, 1993], hydrodynamical processes [Aref, 1983; Stolovitzky *et al.*, 1995], atomic and nuclear physics [Yamamoto & Kaneko, 1993], and solid-state semiconductor structures that are fundamental devices in nanoscience and nanotechnology [Lai *et al.*, 1992a; De Moura *et al.*, 2002].

The presence of external perturbations, namely dissipation [Motter & Lai, 2001; Seoane *et al.*, 2006], dealing with more realistic situations appear in several physical phenomena [Motter *et al.*, 2003]. Also, the presence of noise in open flows has been of interest in recent works [Do & Lai, 2003, 2004] in order to study superpersistent chaotic transients. The study of the effects of noise on a classical chaotic scattering has been carried out in [Mills, 2005; Seoane & Sanjuán, 2008]. The main goal of this paper is to address two new issues: a scaling law between the exponential decay rate of the particles in the scattering region versus the dissipative parameter and a numerical analysis of the fractal dimension for the noisy case.

This manuscript is organized as follows. Section 2 gives a complete description of the models: a two-dimensional map with escapes and the Hénon–Heiles Hamiltonian. In Sec. 3, we provide a study of the effects of dissipation in the dynamics of particles escaping from the scattering region. In Sec. 4, the effects of noise in both systems, the map with uniform noise and the flow with white Gaussian noise, are discussed. Conclusions and a discussion of the main results of this paper are presented in Sec. 5.

2. Model Description

We now introduce the prototype models we use during this paper to show the dynamical behavior of particles in chaotic scattering problems. For this

purpose and in order that our results have a general character we will use both, a map and a flow.

2.1. Map

We use the two-dimensional map used by Lau *et al.* [1991].

This map reads

$$\begin{aligned} x_{n+1} &= \lambda \left[\frac{x_n - (x_n + y_n)^2}{4} \right], \\ y_{n+1} &= \lambda^{-1} \left[\frac{y_n + (x_n + y_n)^2}{4} \right], \end{aligned} \quad (1)$$

where $\lambda > 1$ is the parameter of the system that plays the role of the energy in a realistic case.

The dynamics of this system becomes nonhyperbolic for $\lambda \leq 6.5$ and hyperbolic for $\lambda \geq 6.5$. This system presents one stable fixed point at the center of a KAM island and one unstable fixed point at $(0, 0)$. The stable fixed point becomes a fixed point attractor when dissipation is introduced. We mostly study this map in the nonhyperbolic regime since in this regime the system is sensitive to any variation in the parameters [Motter & Lai, 2001]. We define the scattering region as the region of points remaining in $x^2 + y^2 < r$, where we take $r = 100$. We assume that an orbit has escaped when it is outside this region.

In Fig. 1, a single trajectory of the map is shown. We can check easily that the particle is trapped in a KAM island and it never escapes [Motter & Lai, 2001]. In Fig. 2 we plot, for $\lambda = 4$, the delay-time function for scattering trajectories. The delay-time function represents the values of the escape times against one of the variables of the system, becoming this variable x for our simulation

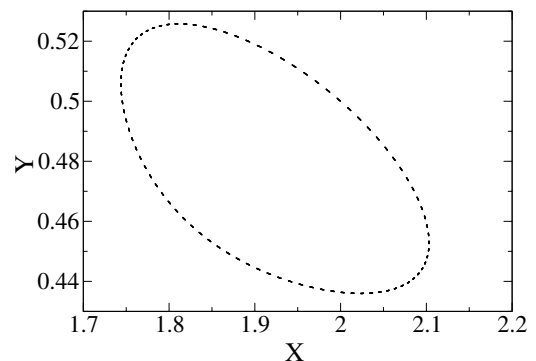


Fig. 1. This figure shows a single trajectory of the two-dimensional map for $\lambda = 4$, where the initial condition is at the point $(x_0, y_0) = (2, 0.5)$.

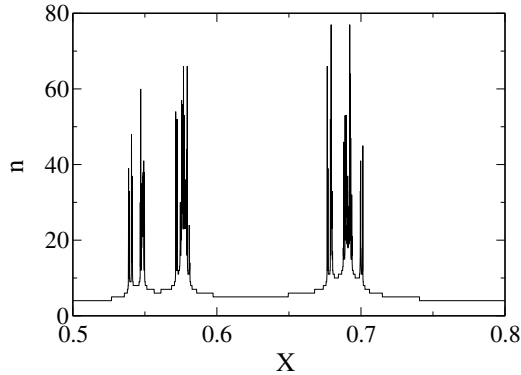


Fig. 2. This figure shows, for $\lambda = 4$ the delay-time function for scattering trajectories. To generate it, $N = 500$ particles are chosen at $y = -2$ with x varying systematically from 0.5 to 0.8. We observe typical features of chaotic scattering: the function contains both smooth parts and discontinuities and, in fact, they are singular on a fractal set.

convenience. It is well known that the fractal dimension of the set of singularities of the scattering function is close to one for the nonhyperbolic case [Lau *et al.*, 1991].

2.2. Flow

We use as a paradigmatic model, the Hénon–Heiles system, as shown in [Aguirre *et al.*, 2001].

The Hénon–Heiles system is described by the Hamiltonian

$$H = \frac{1}{2}(\dot{x}^2 + \dot{y}^2) + \frac{1}{2}(x^2 + y^2) + x^2y - \frac{1}{3}y^3, \quad (2)$$

which defines the motion of a unit mass particle in the two-dimensional potential

$$V(x, y) = \frac{1}{2}(x^2 + y^2) + x^2y - \frac{1}{3}y^3. \quad (3)$$

The system was originally presented in 1964 [Hénon & Heiles, 1964] and for an appropriate value of the total energy, it is used as a paradigmatic system with escapes in Dynamical Astronomy. Two main types of motion exist for different values of the energy: bounded and unbounded motion. There is a threshold value of the energy, called *escape energy*, $E_e = 1/6 = 0.1666$, for which the particle might escape for values of energy above it. In this case, the system presents triangular symmetry with three different exits for which the particles may escape (see, for example, [Seoane *et al.*, 2006; Hénon & Heiles, 1964; Aguirre *et al.*, 2001]). The

equations of motion read

$$\begin{aligned} \ddot{x} + x + 2xy &= 0, \\ \ddot{y} + y + x^2 - y^2 &= 0. \end{aligned} \quad (4)$$

For our simulations, we launch the scattering particles from within the scattering region and examine their escaping trajectories. In particular, the particles are distributed on a vertical line segment centered at $(x, y) = (0, 0)$ and they start their motions in different directions. That is, the subspace in the phase space from which scattering particles are initiated can be denoted by (y, θ) , where θ is the angle of the initial velocity with respect to the x -axis. Figure 3 shows a typical trajectory with $E = 0.2$, where the particle spends a finite amount of time in the scattering region bouncing back and forth among the three potential peaks, before escaping through one of the exits. A basic property of the Hénon–Heiles system is the existence of a class of highly unstable periodic orbits for $E > E_e$, called the *Lyapunov orbits* [Contopoulos, 1990], which live near the border of the scattering region. When a trajectory crosses one of these periodic orbits from inside, it scatters off to infinity. The Lyapunov orbits thus provide a meaningful criterion for measuring the delay times of particles in the scattering region even when the system is dissipative [Contopoulos, 1990].

Figure 4 shows, for $E = 0.19$, the delay-time function for scattering trajectories, where we have chosen $n = 500$ particles at $y = 0$ with initial direction θ varying systematically from 0 to 0.05. As in the map case, typical features of chaotic scattering appear.

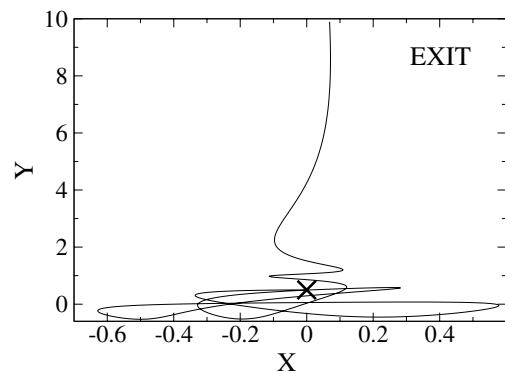


Fig. 3. This figure shows a single trajectory of the Hénon–Heiles system described in Eq. (4). The energy value is $E = 0.19$ where the initial condition is at the point $(x_0, y_0) = (0, 0.5)$, with $\theta_0 = \pi$.

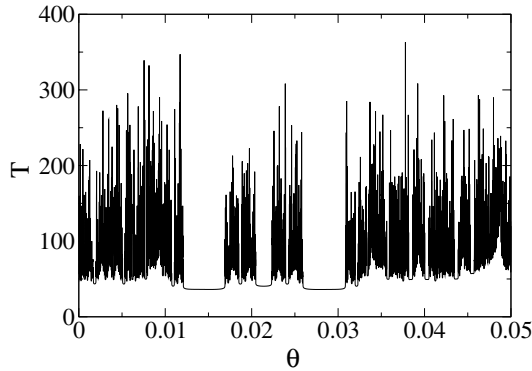


Fig. 4. Typical delay-time function in the Hénon–Heiles system with chaotic scattering for an energy value $E = 0.19$. We have chosen $n = 500$ particles at $y = 0$ with initial direction θ varying systematically from 0 to 0.05. We observe, as in the map case, typical features of chaotic scattering.

The phase space in open hamiltonian systems with three or more exits has a very rich fractal structure. Our system also has a strong topological property, the Wada property. This topological property has been shown in several dynamical systems, the Hénon–Heiles system [Aguirre *et al.*, 2001]. Other references where Wada basins, in other dynamical systems can be found are [Poon *et al.*, 1996; Kennedy & Yorke, 1991; Nusse & Yorke, 1996a, 1996b; Sanjuán *et al.*, 1997; Toroczkai *et al.*, 1997; Sweet *et al.*, 1999; Nusse & Yorke, 2000; Aguirre & Sanjuán, 2002].

3. Escaping Dynamics in Scattering Systems with Dissipation

We now focus on the study of the scattering systems when dissipation is introduced into the system. We

analyze the effects of dissipation in both, the map and the flow shown in the previous section.

For the map case, we introduce the parameter ν , which is responsible of the nonconservative behavior of our previous map. After that, the dissipative two-dimensional map [Motter & Lai, 2001] reads:

$$\begin{aligned} x' &= \lambda \left[\frac{x - (x + y)^2}{4} - \nu(x + y) \right], \\ y' &= \lambda^{-1} \left[\frac{y + (x + y)^2}{4} \right], \end{aligned} \tag{5}$$

where ν is the dissipative parameter. The dissipative version of the map ($\nu > 0$) is a convenient model for studying the effect of weak dissipation on chaotic scattering [Motter & Lai, 2001].

Figure 5(a) shows, for $\nu = 5 \times 10^{-3}$, a typical trajectory in which the particle is trapped, falling into the attractor located at the center of the island. In Fig. 5(b) we plot the delay time function for the dissipative case with $\nu = 5 \times 10^{-3}$. This also suggests, as in the conservative case, a sensitive dependence on initial conditions, the hallmark of chaotic scattering.

We are also interested in the dependence on time of the survival probability of the particles in the scattering region. In hamiltonian systems regular motions are very typical and fundamental. The most classical examples are motions on Kolmogorov–Arnold–Moser (KAM) tori [Moser, 1973; Karney, 1983; Lai *et al.*, 1992b]. This kind of motion characterizes the chaotic scattering in *hyperbolic* and *nonhyperbolic* cases. In hyperbolic chaotic scattering, all the periodic orbits are unstable and

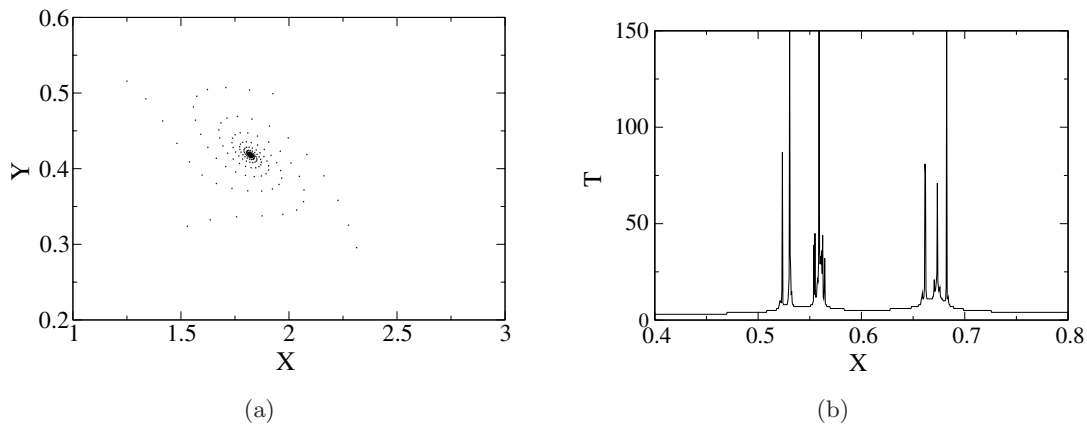


Fig. 5. (a) Single trajectory of the dissipative map for $\lambda = 4$ and $\nu = 5 \times 10^{-3}$ with initial condition $(x_0, y_0) = (2, 0.5)$. We observe that the particle falls into the attractor located at the center of the KAM island. (b) Typical delay-time function for the map in the dissipative case. We easily observe both, smooth and discontinuous parts, which are typical in a fractal set.

there are no KAM tori in the phase space. In this case, the particle decay law is exponential. On the contrary, in nonhyperbolic chaotic scattering, KAM tori coexist with chaotic saddles, which typically results in algebraic decay in the survival probability of a particle in the scattering region. Here we review how dissipation affects the nonhyperbolic regime. Previous works [Motter & Lai, 2001; Seoane *et al.*, 2006; Seoane *et al.*, 2007] have analyzed the effect of weak dissipation in the survival probability of the particles in a nonhyperbolic regime. The authors, in [Motter & Lai, 2001; Seoane *et al.*, 2006; Seoane *et al.*, 2007], found that the algebraic decay law is structurally unstable in the sense that it immediately becomes exponential in the presence of some amount of dissipation, no matter how small it is. Figure 6 shows evidence of this fact in which we launch the particles as we described in the previous section.

We find this exponential law relationship between the fraction of particles remaining in the scattering region and the escape time, $R(n) \sim e^{-\gamma n}$, where $1/\gamma$ is the inverse of the coefficient of the decay law commonly called characteristic time. In Fig. 6 we observe the exponential behavior due to the effects of the dissipation. For convenience, we choose initial conditions from the horizontal line $y_0 = -2$ and $x \in (0.5, 0.6)$ with parameter values $\lambda = 4$, $\nu = 0$ and $\epsilon = 0.5$. The change in the decay law from algebraic to exponential is due to the fact that dissipation destroys the KAM islands converting them into attractors and as a consequence the algebraic law into an exponential law. Heuristic arguments on this point are shown in [Motter & Lai, 2001]. Another important point of the effects of

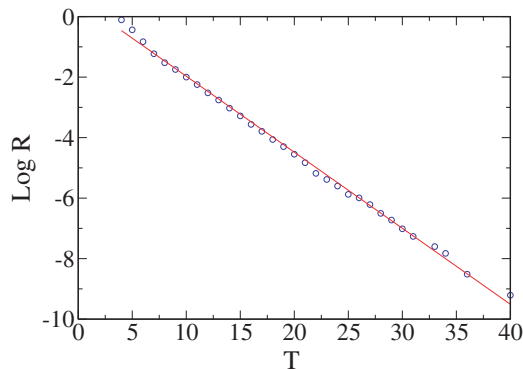


Fig. 6. Decay law for the particles remaining in the scattering region. R denotes the fraction of particles leaving from the scattering region. In the figure we observe the exponential behavior due to the effect of dissipation. Here, we are shooting 500 particles with $\lambda = 4$ and $y_0 = -2$.

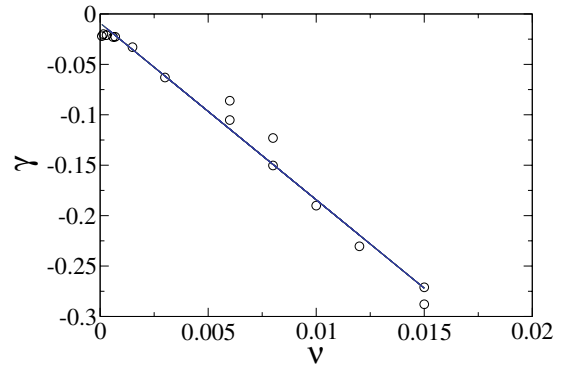


Fig. 7. In this figure, we plot the coefficient of the exponential law, γ , of the scattering particles against the dissipative parameter, ν . We choose, as a parameter, $\lambda = 4$. We observe a linear scaling relationship between γ and ν .

dissipation is the search of the scaling laws between the characteristic parameters of the system. For this purpose we have fixed $\lambda = 4$ for the map. If we plot the coefficient of the exponential γ versus the dissipative parameter, ν , we find, approximately, a linear scaling which is one of the main results of this paper. Figure 7 shows the evidence of this fact. This result is very important in the sense that we can predict (for one specific system) the evolution of the particles in the scattering region. Finally, the fractal dimension of the set of singularities of the scattering function versus the dissipative parameter ν , presents a crossover behavior as shown in [Seoane *et al.*, 2007]. In this work the authors stated that the rate of decrease of the dimension is relatively large initially but, as the dissipation parameter passes through a critical value ν_c , the rate is reduced significantly and becomes nearly zero for $\nu > \nu_c$, becoming ν_c the crossover point.

We now study the same phenomenon for the flow. When dissipation is introduced into the system according to [Seoane *et al.*, 2006], the equations of motion read:

$$\begin{aligned} \ddot{x} + x + 2xy + \mu\dot{x} &= 0, \\ \ddot{y} + y + x^2 - y^2 + \mu\dot{y} &= 0, \end{aligned} \quad (6)$$

where μ is the dissipative parameter.

In this case the stable fixed point located at $(0, 0)$ becomes an attractor, which is easily observed in Fig. 8(a). In order to compute the delay-time function we shoot 500 particles with energy $E = 0.2$ from $(x_0, y_0) = (0, 0.5)$ and $\theta \in (0, 2\pi)$, becoming $\mu = 10^{-3}$, which we plot in Fig. 8(b), observing that it also has a fractal structure as in the map case. On the other hand, the fraction of particles remaining

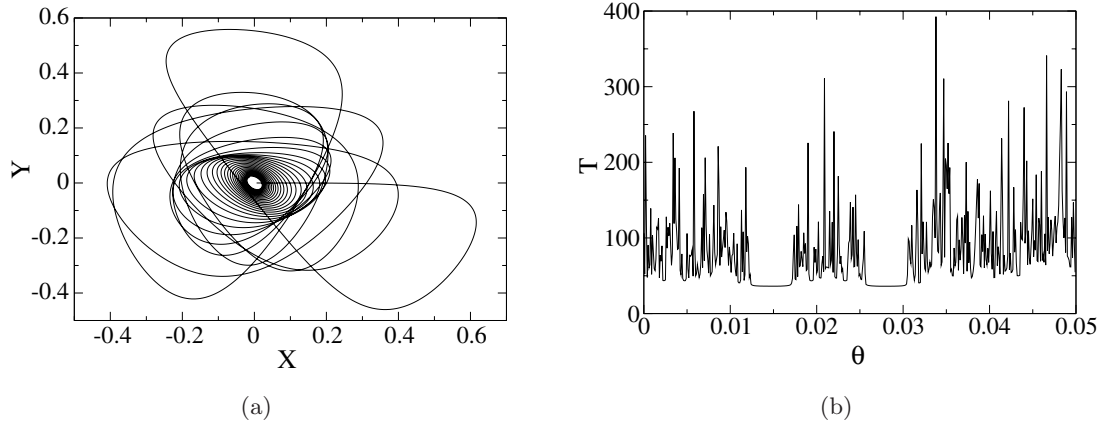


Fig. 8. (a) This figure shows a single trajectory of the Hénon–Heiles system with weak dissipation (described in Eq. (6)). The parameter values are $E = 0.195$ and $\mu = 10^{-3}$, where the initial condition is at the point $(x_0, y_0) = (0, 0.5)$, with $\theta_0 = \pi$. (b) Typical delay-time function for the flow in the dissipative case.

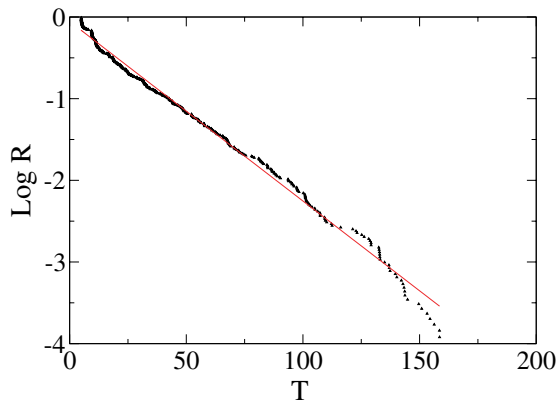


Fig. 9. Exponential decay law for the particles remaining in the scattering region from the flow. R denotes the fraction of particles remaining in the scattering region. Here, we are shooting 500 particles with energy $E = 0.2$ from $(x_0, y_0) = (0, 0.5)$ and $\theta \in (0, 2\pi)$. Dissipative parameter is $\mu = 10^{-3}$.

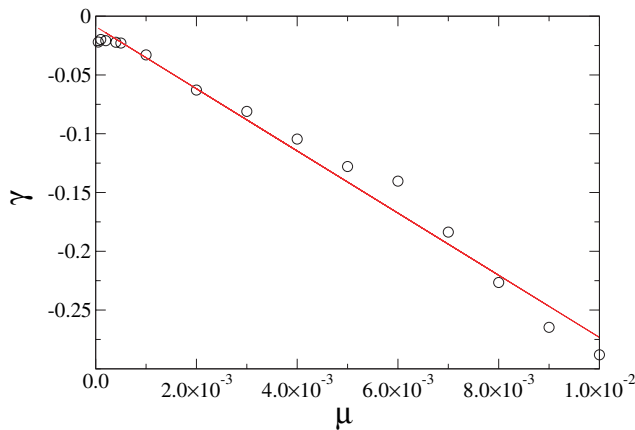


Fig. 10. Plot, for the flow of the coefficient of the exponential law, γ , versus μ . The value of the energy is: $E = 0.19$. We observe, approximately, a linear relation between γ and μ .

in the scattering region, R , versus the escape time, T , is plotted in Fig. 9. In this *log* plot we easily observe the exponential behavior of the decay law, $R(t) \sim e^{-\gamma t}$. The behavior is quite similar as in the case of the map.

If we now plot, for the flow, the coefficient of the exponential law in the survival probability of the particles in the scattering region, γ , against, μ , we obtain a similar scaling law as in the case of the map as shown in Fig. 10.

4. Escaping Dynamics in Noisy Scattering Systems

It has been established in [Seoane & Sanjuán, 2008] that in the presence of noise the particles escape very fast from the scattering region independently of the chosen noise. In order to illustrate the effects of noise we introduce the noisy version of the map and the flow, analyzing both of them.

For the map the equations of motion read:

$$\begin{aligned} x_{n+1} &= \lambda \left[\frac{x_n - (x_n + y_n)^2}{4} - \nu(x_n + y_n) \right] + u_n, \\ y_{n+1} &= \lambda^{-1} \left[\frac{y_n + (x_n + y_n)^2}{4} \right] + v_n, \end{aligned} \tag{7}$$

where u_n and v_n are noise. At each time n , the values of u_n and v_n are chosen independently and randomly from uniform probability distribution functions $U(u)$ and $V(v)$ given by,

$$U(u) = \begin{cases} \frac{1}{2u_0} & \text{if } |u| < u_0, \\ 0 & \text{if } |u| \geq u_0, \end{cases} \tag{8}$$

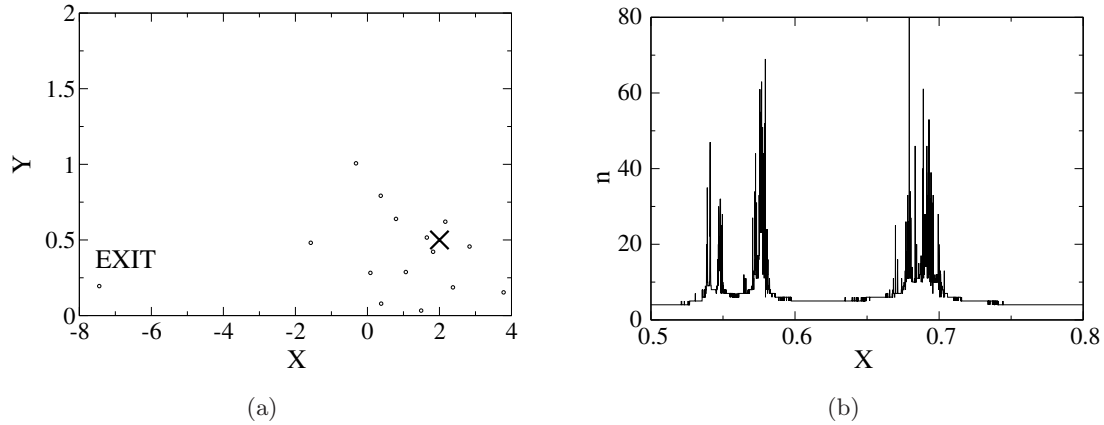


Fig. 11. (a) A trajectory of the two-dimensional map for parameters value $\lambda = 4$ and $\epsilon = 0.2$ where the initial condition is at the point $(x_0, y_0) = (2, 0.5)$ in which the particles are escaping after several iterations due to the noise effect. (b) The typical delay-time function for the noisy case.

$$V(v) = \begin{cases} \frac{1}{2v_0} & \text{if } |v| < v_0, \\ 0 & \text{if } |v| \geq v_0. \end{cases} \quad (9)$$

For convenience we take $u = v = \epsilon$.

In Fig. 11(a) we plot a single trajectory for parameter values $\lambda = 4$ and $\epsilon = 0.2$, where the initial condition is at the point $(x_0, y_0) = (2, 0.5)$. We easily see that the particles are escaping after several iterations due to the noise effect. We also observe that noise destroys the KAM islands and the particles escape very fast from the scattering region. Figure 11(b) shows the typical delay-time function for the noisy case which also contains both, smooth and discontinuous parts. Other characteristic point of the effects of the noise is in the survival probability of the particles scattered in the scattering region. In [Seoane & Sanjuán, 2008] the authors

found an exponential law relationship between the fraction of particles remaining in the scattering region and the escape time, $R(t) \sim e^{-\gamma t}$, showing that this is independent of the chosen noise.

We review now the situation for the flow case in which we introduce white Gaussian noise, for which the equations of motion read as follows:

$$\begin{aligned} \ddot{x} + x + 2xy + \alpha \dot{x} &= \sqrt{2\epsilon} \xi(t), \\ \ddot{y} + y + x^2 - y^2 + \beta \dot{y} &= \sqrt{2\epsilon} \eta(t), \end{aligned} \quad (10)$$

with ϵ is the intensity of the noise and $\xi(t)$ and $\eta(t)$ are random variables. For convenience, we fix $\alpha = \beta = \mu$, where μ is the dissipative parameter. Since we are working with stochastic differential equations we will take the numerical integration explained in [Kloeden & Platen, 1999].

Figure 12(a) shows a typical trajectory of this system for parameter values: $E = 0.19$ and

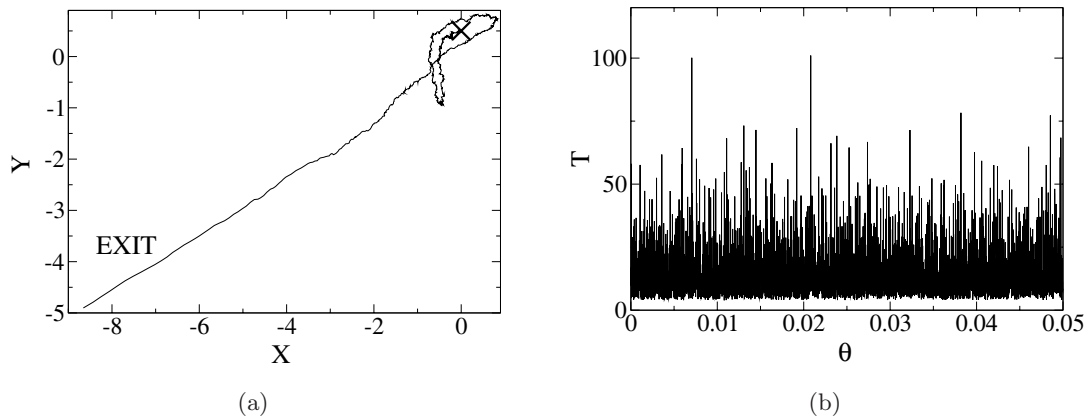


Fig. 12. (a) This figure shows a trajectory of the Hénon–Heiles system with noise intensity $\epsilon = 5 \times 10^{-3}$. The parameter values are $E = 0.19$ and $\mu \geq 0$, where the initial condition is at the point $(x_0, y_0) = (0, 0.5)$, with $\theta_0 = \pi$. Notice that when noise is introduced, the particle escapes faster than in the noiseless case. (b) Typical delay-time function for the Hénon–Heiles system in the presence of noise.

$\epsilon = 5 \times 10^{-3}$. For convenience, we launch particles from within the scattering region and examine the escaping trajectories. In particular, the particles are shot from the vertical line segment centered at $(x_0, y_0) = (0, 0.5)$ with angle with respect to the x -axis to be $\theta_0 = \pi$. The addition of noise shows a classical trajectory in a noisy environment (similar to a random walk) helping the particle to escape earlier than in the noiseless case. The typical delay-time function for the Hénon–Heiles system with $\epsilon = 5 \times 10^{-3}$ is plotted in Fig. 12(b).

As is well known, the addition of weak dissipation does not affect the structural stability of the Wada basins [Seoane *et al.*, 2006]. On the contrary as it is also known, if we introduce a small amount of noise, the topology of the Wada basins is destroyed and the phase space is smeared as shown in [Seoane & Sanjuán, 2008].

4.1. Fractal dimension

One of the main objectives addressed in this paper is a thorough analysis of the fractal dimension of the set of singularities of the scattering function in the presence of noise. As we mentioned in the previous section, for a scattering system, a quantity of physical interest is the scattering function or the delay-time function, which gives the dependence of some physical variables after the scattering on some input variables (e.g. the impact parameter) before the scattering. Scattering functions can be experimentally measured, from which information about the interior of the scattering system can be inferred. For a chaotic scattering system, a scattering function typically contains an uncountably infinite number of singularities [Bleher *et al.*, 1990; Bleher *et al.*, 1989]. For nonhyperbolic chaotic scattering, the fractal dimension of the set of singularities in the scattering function is $D = 1$ [Lau *et al.*, 1991]. This is a direct consequence of the underlying algebraic-decay law, and can be seen intuitively by considering a zero-Lebesgue-measure Cantor set that has $D = 1$. Start with the unit interval $[0, 1]$. Remove the open middle third interval. From each of the two remaining intervals remove the middle fourth interval. Then from each of the four remaining intervals remove the middle fifth, and so on. At the n th stage of the construction, there are $N = 2^n$ subintervals, each of length: $\delta_n = [2/(n+2)]2^{-n}$. The total length of all subintervals $\delta_n N \sim n^{-1}$ goes to zero *algebraically* as $n \rightarrow \infty$. In order to cover the set with intervals of size δ_n , the required

number of intervals is $N(\delta) \sim \delta^{-1}(\ln \delta^{-1})^{-1}$. The box-counting dimension of the set is then $D = \lim_{\delta \rightarrow 0} \ln N(\delta) / \ln \delta^{-1} = 1$. Note that, D is the exponent of the dependence $N(\delta) \sim 1/\delta^D$, to which the weak logarithmic dependence does not contribute. However, it is the logarithmic term which is responsible for ensuring that the Lebesgue measure is zero: $\delta N(\delta) \sim (\ln \delta^{-1})^{-1} \rightarrow 0$ as $\delta \rightarrow 0$. In a more general setting, if at each stage a fraction $\eta_n = a/(n+c)$, where a and c are constants, is removed from the middle of each of the 2^n remaining intervals, then $N(\delta) \sim (1/\delta)[\ln(1/\delta)]^{-a}$. In this case, the slope of the curve $\ln N(\delta)$ versus $\ln \delta^{-1}$, which is $d \ln N(\delta) / d(\ln \delta^{-1})$, is always less than 1 for small δ , but it approaches 1 logarithmically as $\delta \rightarrow 0$. Thus, the result $D = 1$ still holds. A practical implication is that for fractals whose general characters are similar to those for this example, an accurate numerical estimation of the dimension requires going to very small scales and, as such, any numerical estimation of the dimension over a finite range of scales will be an underestimate. As the scale is decreased, the numerically determined value of the dimension increases toward 1.

In a chaotic scattering system, particles are launched from a line segment straddling the stable manifold of the chaotic saddle. There is then an interval of input variables which lead to trajectories that remain in the scattering region for at least a duration of time, say T_0 . By time $2T_0$ a fraction η of these particles leave. If the initial conditions of these escaping particles are all located in the middle of the original interval, there are then two equal-length subintervals of the input variable which lead to trajectories that remain for at least time $2T_0$. By time $3T_0$ an additional fraction η of the particles, whose initial conditions are located in the middle of the two subintervals remaining at time $2T_0$, escape. There are then four subintervals, particles initiated from which can remain in the scattering region for time at least $3T_0$, and so on. The resulting set is a Cantor set of Lebesgue measure zero on which particles never escape. The box-counting dimension of the Cantor set is given by

$$D = \frac{\ln 2}{\ln \left[\frac{1-\eta}{2} \right]^{-1}}.$$

In the conservative case, if the scattering is non-hyperbolic, because of the algebraic decay: $P(t) \sim t^{-z}$, the fraction η is no longer a constant: it varies at each stage of the construction of the Cantor set.

At the n th stage (n large), the fraction η_n is approximately given by $\eta_n \approx -T_0 P^{-1} dP/dt \approx z/n$, which yields a Cantor set with dimension 1, where the quantity a in the mathematical construction of the Cantor set corresponds to the algebraic-decay exponent z . For conservative hyperbolic chaotic scattering, particles escape exponentially from the scattering region: $P(t) \sim e^{-\gamma t}$, where the decay rate γ is related to the fraction η as $\gamma = T_0^{-1} \ln(1 - \eta)^{-1}$. In [Seoane *et al.*, 2007] the authors focused their study in the characterization of the fractal dimension in the dissipative case finding a crossover behavior as indicated in Sec. 3. Here we address the effect of noise to the fractal dimension in both systems, the map and the flow.

4.1.1. Fractal dimension for the map

The fractal dimension of the set of singularities would be interesting to know once noise is introduced into the system and it is our focus of attention here.

Figure 11(b) shows, for $\lambda = 4$ and ($\epsilon = 0.05$), the delay-time function for scattering trajectories, where we have chosen, $N = 500$ particles at $y = -2$ with x varying systematically from 0.5 to 0.8. At the scale shown, the two plots exhibit qualitatively similar features. However, the fractal dimensions of the set of singularities in the two functions are not equal. In the conservative case, the value is close or slightly less than the unity and equal or slightly larger than the unity, $D \geq 1$, once a small amount of noise is introduced. To demonstrate this, we use the uncertainty algorithm [Grebogi *et al.*, 1983] to numerically calculate the fractal dimension.

To perform the dimension calculation, we use the uncertainty algorithm [Grebogi *et al.*, 1983]. In particular, we choose a line segment defined by $y_0 = -2$ from which trajectories are launched toward the scattering region about $(x, y) = (0, 0)$. For a given initial condition \mathbf{x}_0 on the line segment, a perturbed initial condition $\mathbf{x}_0 + \epsilon$ can be chosen, where ϵ is the amount of perturbation. If the two trajectories from the initial conditions escape (say when $\sqrt{x^2 + y^2} > 10$) in the same number of iterations, or if both trajectories approach the same attractor, the two initial conditions are *certain* with respect to the perturbation ϵ . Otherwise, if the trajectories escape in different numbers of iterations, or if the trajectories approach distinct attractors, the initial conditions are *uncertain* with respect to the perturbation ϵ . Among a large number of initial conditions, the fraction of uncertain initial conditions $f(\epsilon)$ scales algebraically with ϵ as $f(\epsilon) \sim \epsilon^{1-D}$, or $f(\epsilon)/\epsilon \sim \epsilon^{-D}$, where D is the fractal dimension [Grebogi *et al.*, 1983] of the set of singularities in a scattering function defined on the initial line segment. Figure 13(a) shows, for $\nu = 0$ and $\epsilon = 0.2$, the algebraic scaling of $f(\epsilon)/\epsilon$ with ϵ . We obtain $D = 1.02 \pm 0.01$. [In the actual computation of $f(\epsilon)$, we increase the number of random initial conditions until the number of uncertain initial conditions reaches a prescribed value (say 500)]. If we plot the variation of the fractal dimension, D , versus noise amplitude, ϵ , we find that for large values of noise, $\epsilon \geq \epsilon_c$, the fractal dimension D keeps a little bigger than the unity as it occurs in noisy systems. Figure 13(b) shows this phenomenon in which it can be observed that it takes place for the critical value of epsilon. It indicates that the

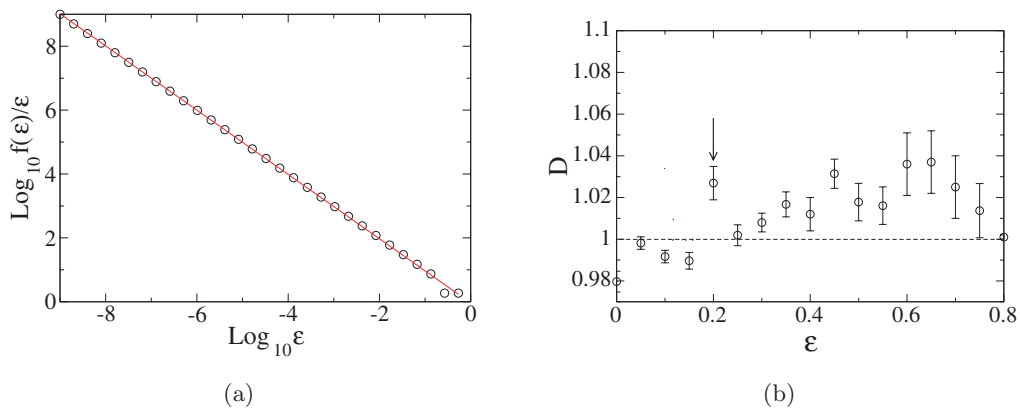


Fig. 13. (a) For the map, with $\lambda = 4$, algebraic scaling of $f(\epsilon)/\epsilon$ versus ϵ for noise amplitude $\epsilon = 0.2$. The fractal dimension is estimated to be $D = 1.02 \pm 0.01$. (b) Dependence of the dimension, D , on the noise amplitude ϵ . We can observe the transition point and the region in which $D \geq 1$. Vertical arrow denotes the value of the intensity of noise for which the particles escape very fast.

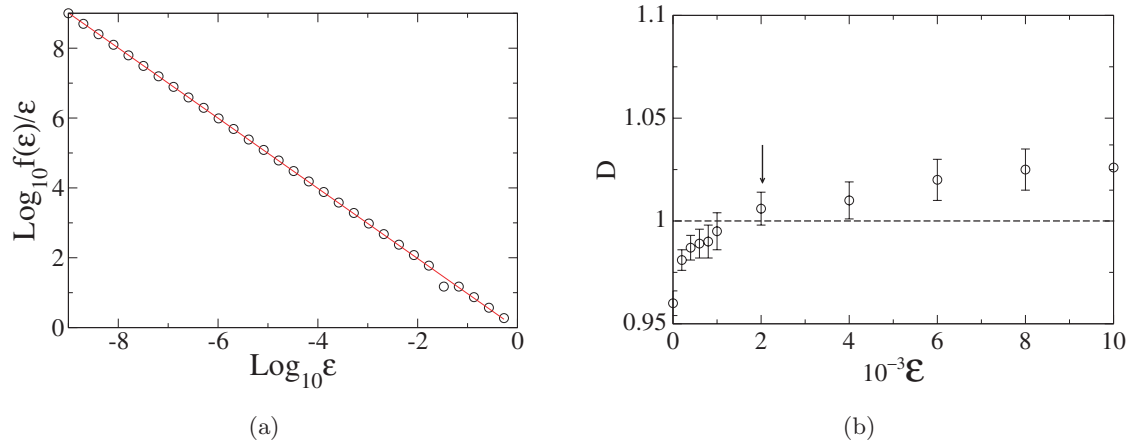


Fig. 14. (a) For the flow, with $E = 0.19$, algebraic scaling of $f(\epsilon)/\epsilon$ versus ϵ for noise amplitude $\epsilon = 10^{-3}$. The fractal dimension is estimated to be $D = 0.99 \pm 0.01$. (b) Dependence of the dimension, D , on the noise amplitude ϵ . We can observe the transition point and the region in which $D \geq 1$ as occurs in the map case. Vertical arrow denotes the value of the intensity of noise for which the particles escape very fast.

particles are escaping very fast from the scattering region.

4.1.2. Fractal dimension for the flow

Figure 12(b) shows, for $E = 0.19$ and $\epsilon = 0.005$, the delay-time function for scattering trajectories, where we have chosen $N = 500$ particles at $y = 0$ with initial direction θ varying systematically from 0 to 0.05.

The fractal dimension of the set of singularities in a scattering function can be calculated by using the same uncertainty algorithm. Figure 14(a) shows, for $E = 0.19$ and $\epsilon = 10^{-3}$, the algebraic scaling of $f(\epsilon)/\epsilon$ with ϵ , where initial conditions are chosen from the line segment outside the scattering region defined by $(x_0, y_0) = (0, 1)$ and $\Theta \in (0, 2\pi)$, where Θ is the shooting angle with respect to the x -axis. We obtain $D = 0.99 \pm 0.01$. If we plot, as in the case of the map, the variation of D versus the noise amplitude ϵ we find the same phenomenon in which $D \geq 1$ which is typical in noisy systems [Fig. 14(b)].

5. Conclusions and Discussion

In conclusion, by using as prototype models, a two-dimensional map with escapes and the Hénon–Heiles Hamiltonian, we have shown the influence of introducing dissipation and noise in the behavior of the scattering system. We have shown that the decay rate of the scattering particles follows an exponential law, in the same way that it was known

for a two-dimensional map. These decay rates indicate that the particles escape from the scattering region faster or slower depending on noise or dissipation as added, respectively. We also have shown a scaling law between the coefficient of the exponential law against the dissipative parameter. We have provided numerical support for this fact by computing the fractal dimension of the set of singularities of the scattering function obtaining that its value is less than one for the dissipative case and one for the noisy case. In physical contexts, our work can appear in advective dynamics of inertial particles in open chaotic flows which also has implications to problems of current concern such as the transport and trapping of chemically or biologically active particles in large-scale flows. We expect this work to be useful for a better understanding of chaotic scattering phenomena because our models are paradigmatic systems and the results can be, in principle, generalized for higher-dimensional problems and for any open dynamical system.

Acknowledgments

This work was supported by the Spanish Ministry of Education and Science under project number FIS2006-08525 and by Universidad Rey Juan Carlos and Comunidad de Madrid under project number URJC-CM-2007-CET-1601. J. Seoane acknowledges financial support and warm hospitality received at Arizona State University where part of this work was carried out.

References

- Aguirre, J., Vallejo, J. C. & Sanjuán, M. A. F. [2001] “Wada basins and chaotic invariant sets in the Hénon–Heiles system,” *Phys. Rev. E* **64**, 066208–066208-11.
- Aguirre, J. & Sanjuán, M. A. F. [2002] “Unpredictable behavior in the Duffing oscillator: Wada basins,” *Physica D* **171**, 41–51.
- Aref, H. [1983] “Integrable, chaotic, and turbulent vortex motion in two-dimensional flows,” *Annu. Rev. Fluid. Mech.* **15**, 345–389.
- Bleher, S., Ott, E. & Grebogi, C. [1989] “Routes to chaotic scattering,” *Phys. Rev. Lett.* **63**, 919–922.
- Bleher, S., Grebogi, C. & Ott, E. [1990] “Bifurcation to chaotic scattering,” *Physica D* **46**, 87–121.
- Boyd, P. T. & McMillian, S. L. W. [1993] “Chaotic scattering in the gravitational three-body problem,” *Chaos* **3**, 507–523.
- Chernikov, A. A. & Schmidt, G. [1993] “Chaotic scattering and acceleration of particles by waves,” *Chaos* **3**, 525–528.
- Contopoulos, G. [1990] “Asymptotic curves and escapes in Hamiltonian systems,” *Astron. Astrophys.* **231**, 41–55.
- de Moura, A. P. S., Lai, Y.-C., Akis, R., Bird, J. P. & Ferry, D. K. [2002] “Tunneling and nonhyperbolicity in quantum dots,” *Phys. Rev. Lett.* **88**, 236804–236804-4.
- Ding, M., Grebogi, C., Ott, E. & Yorke, J. A. [1990] “Transition to chaotic scattering,” *Phys. Rev. A* **42**, 7025–7040.
- Do, Y. & Lai, Y. C. [2003] “Superpersistent chaotic transients in physical space: Advective dynamics of inertial particles in open chaotic flows under noise,” *Phys. Rev. Lett.* **91**, 224101–224101-4.
- Do, Y. & Lai, Y. C. [2004] “Stability of attractors by inertial particles in open chaotic flows,” *Phys. Rev. E* **70**, 036203–036203-10.
- Grebogi, C., McDonald, S. W., Ott, E. & Yorke, J. A. [1983] “Final state sensitivity: An obstruction to predictability,” *Phys. Lett. A* **99**, 415–418.
- Hénon, M. & Heiles, C. [1964] “The applicability of the third integral of motion: Some numerical experiments,” *Astron. J.* **69**, 73–79.
- Hénon, M. [1988] “Chaotic scattering modelled by an inclined billiard,” *Physica D* **33**, 132–156.
- Jung, C. [1986] “Poincare map for scattering states,” *J. Phys. A* **19**, 1345–1353.
- Karney, C. F. F. [1983] “Long time correlations in the stochastic regime,” *Physica D* **8**, 360–380.
- Kennedy, J. & Yorke, J. A. [1991] “Basins of Wada,” *Physica D* **51**, 213–225.
- Kloeden, P. E. & Platen, E. [1999] *Numerical Solution of Stochastic Differential Equations* (Springer, NY).
- Lai, Y.-C., Blümel, R., Ott, E. & Grebogi, C. [1992a] “Quantum manifestations of chaotic scattering,” *Phys. Rev. Lett.* **68**, 3491–3494.
- Lai, Y. C., Ding, M., Grebogi, C. & Blümel, R. [1992b] “Algebraic decay and fluctuations of the decay exponent in Hamiltonian systems,” *Phys. Rev. A* **46**, 4661–4669.
- Lau, Y. T., Finn, J. M. & Ott, E. [1991] “Fractal dimension in nonhyperbolic chaotic scattering,” *Phys. Rev. Lett.* **66**, 978–981.
- Mills, P. [2005] “The influence of noise on a classical chaotic,” *Commun. Nonlin. Sci. Numer. Simul.* **11**, 899–906.
- Moser, J. [1973] *Stable and Random Motions in Dynamical Systems* (Princeton University Press, Princeton, NJ).
- Motter, A. E. & Lai, Y.-C. [2001] “Dissipative chaotic scattering,” *Phys. Rev. E* **65**, 015205–015205-4.
- Motter, A. E., Lai, Y. C. & Grebogi, C. [2003] “Reactive dynamics of inertial particles in nonhyperbolic chaotic flows,” *Phys. Rev. E* **68**, 056307–056307-5.
- Nusse, H. E. & Yorke, J. A. [1996a] “Basins of attraction,” *Science* **271**, 1376–1380.
- Nusse, H. E. & Yorke, J. A. [1996b] “Wada basin boundaries and basin cells,” *Physica D* **90**, 242–261.
- Nusse, H. E. & Yorke, J. A. [2000] “Fractal basins boundaries generated by basin cells and the geometry of mixing chaotic flows,” *Phys. Rev. Lett.* **84**, 626–629.
- Ott, E. & Tél, T. [1993] “Chaotic scattering: An introduction,” *Chaos* **3**, 417–426.
- Poon, L., Campos, J., Ott, E. & Grebogi, C. [1996] “Wada basins boundaries in chaotic scattering,” *Int. J. Bifurcation and Chaos* **6**, 251–266.
- Sanjuán, M. A. F., Kennedy, J., Grebogi, C. & Yorke, J. A. [1997] “Indecomposable continua in dynamical systems with noise: Fluid flow past an array of cylinders,” *Chaos* **7**, 125–138.
- Seoane, J. M., Aguirre, J., Sanjuán, M. A. F. & Lai, Y. C. [2006] “Basin topology in dissipative chaotic scattering,” *Chaos* **16**, 023101–023101-8.
- Seoane, J. M., Sanjuán, M. A. F. & Lai, Y. C. [2007] “Fractal dimension in dissipative chaotic scattering,” *Phys. Rev. E* **76**, 016208–016208-6.
- Seoane, J. M. & Sanjuán, M. A. F. [2008] “Exponential decay and scaling laws in noisy chaotic scattering,” *Phys. Lett. A* **372**, 110–116.
- Seoane, J. M., Huang, L., Sanjuán, M. A. F. & Lai, Y. C. [2009] “Effects of noise on chaotic scattering,” *Phys. Rev. E* **79**, 047202–047202-4.
- Stolovitzky, G., Kaper, T. J. & Sirovich, L. [1995] “A simple model of chaotic advection and scattering,” *Chaos* **5**, 671–686.
- Sweet, D., Ott, E. & Yorke, J. A. [1999] “Topology in chaotic scattering,” *Nature* **399**, 315–316.
- Toroczka, Z., Károlyi, G., Péntek, Á., Tél, T., Grebogi, C. & Yorke, J. A. [1997] “Wada dye boundaries in open hydrodynamical flows,” *Physica A* **239**, 235–243.
- Yamamoto, T. & Kaneko, K. [1993] “Helium atom as a classical three-body problem,” *Phys. Rev. Lett.* **70**, 1928–1931.